Theoretical Studies of the Modulation of Polymer Electronic and Optical Properties through the Introduction of the Electron-Donating 3,4-Ethylenedioxythiophene or Electron-Accepting Pyridine and 1,3,4-Oxadiazole Moieties

Li Yang,[†] Yi Liao,[‡,§] Ji-Kang Feng,*[,†,‡] and Ai-Min Ren[†]

State Key Laboratory of Theoretical and Computational Chemistry, Institute of Theoretical Chemistry, and College of Chemistry, Jilin University, Changchun 130023, People's Republic of China, and Institute of Functional Material Chemistry, Faculty of Chemistry, Northeast Normal University, Changchun 130024, People's Republic of China

Received: March 24, 2005; In Final Form: July 8, 2005

One serious problem associated with polyfluorene and derivatives (PFs) as blue luminescent polymers is the significant energy barrier for hole or electron injections; thus they usually face charge injection and transport difficulties with the currently available cathode and anode materials. The incorporation of an electron-donating or -accepting unit is expected to improve the recombination of the charge carriers. In this paper, we apply quantum-chemical techniques to investigate three fluorene-based copolymers, copoly(2,5-ethylenedioxythiophene-*alt*-9,9′-dimethylfluorene) (PEF), copoly(2,5-pyridine-*alt*-9,9′-dimethylfluorene) (PPyF), and poly-[(fluorene-2,7-diyl)-*alt*-(1,3,4-oxadiazole-2,5-diyl)] (PFO), in which Δ_{H-L} [the energy difference between the highest occupied molecular orbital (HOMO) and the lowest unoccupied molecular orbital (LUMO), when $n = \infty$], the lowest excitation energies (E_g), ionization potentials (IP), electron affinities (EA), and λ_{abs} and λ_{em} are fine-tuned by the regular insertion of electron-donating unit 3,4-ethylenedioxythiophene (EDOT) or electron-withdrawing units pyridine and 1,3,4-oxadiazole. The results show that the alternate incorporation of electron-donating moiety EDOT increases the HOMO energy and thus reduces the IPs, and consequently the hole injection was greatly improved. On the other hand, even though both kinds of charge carriers will improve the electron-accepting ability, the results show that electron-withdrawing moieties greatly facilitate the electron-transporting. Especially in PFO, the highly planar structural character resulted from the strong push−pull effect between the fluorene ring and the 1,3,4-oxadiazole ring and a weak interaction between the nitrogen and oxygen atoms in 1,3,4-oxadiazole ring and the hydrogen atom of the fluorene ring, significantly lowering the LUMO energy levels and thus improve the electron-accepting and transporting properties by the low LUMO energy levels.

1. Introduction

Conjugated polymers and oligomers offer new opportunities in information technology since they can be used as active materials in light-emitting diodes (LED),[1,2] field-effect transistors,[3−6] and plastic solar cells.[7] Until now, the unaccomplished development of efficient and long-lived PLEDs has delayed the commercialization of full-color PLED displays. The exceptional physical properties of conjugated polymers are mainly related to their π-conjugated backbone, which leads to a strong absorption in the UV−visible range and allows the generation of stable and mobile charge carriers to have partial oxidation or reduction.[8−10] With molecular design tools, new monomers were synthesized with the goal to control and tune their optical and electronic properties. Especially, theoretical studies on the electronic structures of polymers have contributed a lot to rationalize the properties of known polymers[11−18] and to predict those of yet unknown ones.[19] Much of the motivation for studying polymers stems from the potential to tailor desirable optoelectronic properties and processing characteristics by manipulation of the primary chemical structure. Thus, it is easy to raise or lower the highest occupied and lowest unoccupied molecular orbital (HOMO and LUMO) levels including conjugation length control, as well as the introduction of electron-donating or -withdrawing groups and electron-deficient heterocycles to the parent chromophore.

The mobilities are important in optimizing the performance of OLED devices; low mobilities enhance the resistance of the device, leading to nonproductive hole or electron injection and consequently a waste of energy, thereby lowering the efficiency. One major problem with polyfluorene derivatives (PFs),[20−23] which have revealed particularly interesting optical and electronic properties and, up to now, is the only family of conjugated polymers that emit colors spanning the entire visible range, is that they are poor charge acceptors. Here, to balance charge carriers by the match-up of the energy levels between introduced layers and between an inner layer and an electrode and to improve the electroluminescence efficiencies, 2,5-ethylenedioxythiophene, pyridine, and 1,3,4-oxadiazole are introduced, acting as hole and electron charge carriers, and three series of π-conjugated copolymers based on the fluorene unit, copoly-(2,5-ethylenedioxythiophene-*alt*-9,9′-dimethylfluorene) (PEF), copoly(2,5-pyridine-*alt*-9,9′-dimethylfluorene) (PPyF),[24] and poly[(fluorene-2,7-diyl)-*alt*-(1,3,4-oxadiazole-2,5-diyl)]-(PFO)[23] (shown in Figure 1) are investigated by density

[†] State Key Laboratory of Theoretical and Computational Chemistry, Institute of Theoretical Chemistry, Jilin University.
[‡] College of Chemistry, Jilin University.
[§] Northeast Normal University.

10.1021/jp0515277 CCC: $30.25
Published on Web 08/09/2005

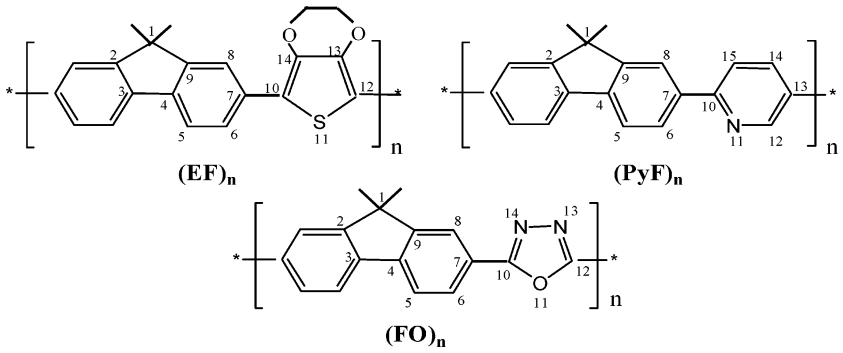

Figure 1. Sketch map of the structures.

functional theory (DFT) methods. A theoretical investigation on the ionization potentials (IP), electron affinities (EA), and band gaps of these polymers is very instrumental in guiding the experimental synthesis, which is the topic of the present work.

The majority of the studies on polymers by first-principles methods consider in fact oligomers. The general strategy is the simulation of a number of oligomers of increasing lengths, such that the properties of the polymers can be inferred by extrapolating the results.[25−34] A distinct advantage of this approach is that it can provide the convergence behavior of the structural and electronic properties of oligomers. Time-dependent density functional theory (TD-DFT) is employed to extrapolate energy gaps of polymers from the lowest calculated excitation energies of their oligomers. It is pointed out that TD-DFT systematically underestimated the excitation energies by 0.2−0.5 eV compared to the experimental results due to the limitation of the current approximate exchange-correlation functionals in correctly describing the exchange-correlation potential in the asymptotic region.[35,36] However, reasonable results can still be expected here, because (1) we use the HF/DFT hybrid functionals B3LYP, which could partially overcome the asymptotic problem,[30,37,38] and (2) we study the homologous fluorene-based cooligomers and polymers, with our interests in their modulation of electronic and optical properties by regular insertion of electron-donating and -withdrawing groups onto the pristine polyfluorene. Since the electronic and optical properties of conjugated oligmers saturate rapidly with chain length, we have considered oligomers of PEF, PPyF, and PFO containing from one to four repeat units.[39]

2. Computational Details

All calculations on the oligomers studied in this work have been performed on the SGI origin 2000 server with the Gaussian 03 program package.[40] Calculations on the electronic ground state were carried out by density functional theory (DFT), B3LYP/6-31G(d). The investigated polymers correspond to copolymers Poly-EF8, Poly-PyF8, and PFOx1 in the literature,[23,24] and the main difference is that the ones under study substitute 9,9-dihexyl with methyl in fluorene rings. It has been proved that the presence of alkyl groups does not significantly affect the equilibrium geometry and thus the electronic and optical properties.[41,42] In the subsequent parts, the calculated values are all compared with the experimental data for their corresponding 9,9-dihexylfluorene copolymers in refs 24 and 25. The copolymer PEF has been investigated by Cornil et al.[39] with semiempirical Hartree−Fock INDO (intermediate neglect of differential overlap) Hamiltonian originally developed by Zerner and co-workers. The cationic and anionic molecules are optimized by UB3LYP/6-31G(d). Since the EA is related to the anionic system whose electron charge distribution becomes much more diffuse and requires the use of a larger basis set (usually including at least one set of diffuse functions), we carry out the single-point calculations for the energies of IP and EA using a 6-31+G(d) basis set, and the results are listed in Table 4.

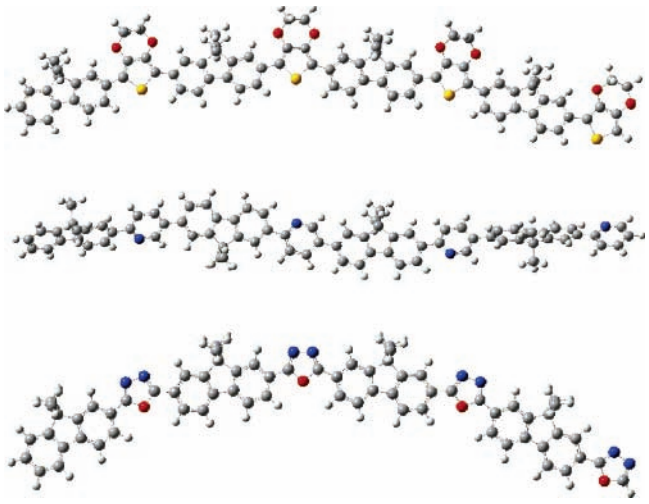

Figure 2. Optimized structures for $(EF)_4$ (top), $(PyF)_4$ (middle), and $(FO)_4$ (bottom) by DFT//B3LYP/6-31G(d).

The energy gap has been estimated two ways, namely, from HOMO−LUMO gap and the lowest excited energies. The transition energies will be calculated at the ground-state geometries by use of TD-DFT/B3LYP calculations, and the results are compared with the available experimental data. The excited geometries were optimized by ab initio CIS/6-31G(d).[43] On the basis of the excited geometries, the emission spectra of part of the molecules are investigated. We employed the linear extrapolation technique in this research, which has been successfully employed to investigate several series of polymers.[30−34,37,39,44] The linearity between the calculated IPs, EAs, Δ_{H-L}s, and E_gs of the oligomers and the reciprocal chain length is excellent for all homologous series of oligomers.

3. Results and Discussion

3.1. Structural Properties of Ground States. The sketch map of the structures for copoly(2,5-ethylenedioxythiophene-*alt*-9,9′-dimethylfluorene) (PEF), copoly(2,5-pyridine-*alt*-9,9′-dimethylfluorene) (PPyF), and poly[(fluorene-2,7-diyl)-*alt*-(1,3,4-oxadiazole-2,5-diyl)] (PFO) is depicted in Figure 1 and the optimized structures by B3LYP/6-31G(d) of $(EF)_4$, $(PyF)_4$, and $(FO)_4$ are plotted in Figure 2. The selected important interring bond lengths and dihedral angles, as well as dipole moments of $(EF)_n$, $(PyF)_n$, and $(PFO)_n$ ($n = 1\sim4$) in the neutral

TABLE 1: Selected Important Interring Dihedral Angles and Distances of $(EF)_n$, $(PyF)_n$, and $(FO)_n$ ($n = 1\sim4$), as Well as Dipole Moments Obtained by B3LYP/6-31G(d) Calculations[a]

$(EF)_n$		F−T	T−F	F−T	T−F	F−T	T−F	F−T	dipole moment (*D*)
$n = 1$	*r*	1.465							2.78
	Φ	21.5							
$n = 2$	*r*	1.463	1.462	1.464					5.66
	Φ	18.9	18.8	21.7					
$n = 3$	*r*	1.463	1.462	1.462	1.462	1.464			8.46
	Φ	19.6	19.4	18.2	19.3	21.5			
$n = 4$	*r*	1.463	1.462	1.462	1.462	1.462	1.462	1.464	10.28
	Φ	20.0	19.3	19.0	18.0	19.5	18.9	22.0	
$(PyF)_n$		F−P	P−F	F−P	P−F	F−P	P−F	F−P	dipole moment (*D*)
$n = 1$	*r*	1.487							1.98
	Φ	18.3							
$n = 2$	*r*	1.487	1.480	1.485					2.01
	Φ	18.7	36.6	15.2					
$n = 3$	*r*	1.484	1.479	1.484	1.479	1.487			3.32
	Φ	17.7	35.9	19.0	36.3	19.4			
$n = 4$	*r*	1.484	1.479	1.485	1.479	1.485	1.479	1.487	3.38
	Φ	18.5	35.9	17.2	36.0	16.4	35.5	19.9	
$(FO)_n$		F−O	O−F	F−O	O−F	F−O	O−F	F−O	dipole moment (*D*)
$n = 1$	*r*	1.457							3.50
	Φ	0.0							
$n = 2$	*r*	1.455	1.455	1.457					5.90
	Φ	0.0	0.0	0.0					
$n = 3$	*r*	1.455	1.455	1.455	1.455	1.457			8.15
	Φ	0.0	0.0	0.0	0.0	0.0			
$n = 4$	*r*	1.455	1.455	1.455	1.455	1.455	1.455	1.457	10.28
	Φ	0.0	0.0	0.0	0.0	0.0	0.0	0.0	

[a] F means the fluorene ring; T is the 2,5-ethylenedioxythiophene; P is the pyridine; O is the 1,3,4-oxadiazole in every molecule.

ground state obtained by DFT//B3LYP/6-31G(d) calculations are listed in Table 1. The results of the optimized structures for all three series of copolymeric molecules show that the bond lengths and bond angles do not suffer appreciable variation with the oligomer size. And it suggests that we can describe the basic structures of the polymers as their oligomers. In fact, because the dihedral angle between two phenyl rings in the fluorene segment of the series of oligomers is fixed by ring bridged atoms, which tend to keep their normal tetrahedral angles in their ring linkage to keep their quasiplanar conformation, the dihedral angles in them are no more than 1°. The biggest torsional angles are Φ(8,7,10,14(15)), the dihedral angles between the two adjacent units, such as the ones between fluorene and EDOT, pyridine, or oxadiazole. The $(FO)_n$ sequence has the best planar conformation in all three series of copolymers with the dihedral angles of almost 0°, due to the strong push−pull effect between the fluorene ring and the 1,3,4-oxadiazole ring, or it could also be explained due to a weak interaction between the nitrogen and oxygen atoms in the 1,3,4-oxadiazole ring and the hydrogen atom of the fluorene ring. Accordingly, the interring distances are the shortest. The ground-state geometry of each oligomer in $(EF)_n$ is more twisted than that in $(FO)_n$ with the interring dihedral angles between fluorene and EDOT around 20°, due to the electron donor properties and increasing steric hindrance by the addition of alkoxy on the thiophene ring, which thus leads to the slightly longer interring distances. In the $(PyF)_n$ sequence, Φ(8,7,10,15) in each oligomer is about 18° and the dihedral angles between each monomer are ∼36°; in other words, the π-conjugated backbone in $(PyF)_n$ is broken by the addition of the pyridine moiety. The results suggest that the six-membered aromatic rings create more steric hindrance than five-membered rings and thus obtain the longest interring bond lengths in the three series. However, even though there are some torsions, the introduction of charge carriers into fluorene still enhance the π-conjugated structures compared with PF, in which the interring torsional angle is ∼36°,[34] especially in $(FO)_n$ and $(EF)_n$.

As observed in Table 1, the dipole moments tend to increase with increasing conjugation lengths in all series. In addition, the dipole moments of the oligomers in $(EF)_n$ and $(FO)_n$ are much larger than that in $(PyF)_n$, ascribed to the presence of more oxygen atoms and the added sulfur or nitrogen atoms. This clearly indicates the influence of different charge carriers on the overall dipole moment.

3.2. Frontier Molecular Orbitals. It will be useful to examine the highest occupied orbitals and the lowest virtual orbitals for these oligomers and polymers because the relative ordering of the occupied and virtual orbitals provides a reasonable qualitative indication of the excitation properties[45] and of the ability of electron or hole transport. Since the first dipole-allowed electron transitions, as well as the strongest electron transitions with largest oscillator strength, correspond almost exclusively to the promotion of an electron from HOMO to LUMO (see section 3.5), we have plotted the electronic density contours of the frontier orbitals of $(EF)_n$, $(PyF)_n$, and $(FO)_n$ ($n = 1\sim4$) by B3LYP/6-31G(d) in Figure 3.

As shown in Figure 3, all the frontier orbitals spread over the whole π-conjugated backbone, although the largest contributions come from the different parts of the chromophores. There is interring antibonding between the bridge atoms, and there is intraring bonding between the bridge carbon atom and its conjoined atoms in the HOMO. On the contrary, there is interring bonding in the bridge single bond and intraring antibonding between the bridge atom and its neighbor in the LUMO. In general, the HOMO possesses antibonding character between the subunits. This may explain the nonplanarity observed for these oligomers in their ground states. On the other hand, the LUMO of all the oligomers generally shows bonding character between the two adjacent subunits. This implies that the singlet excited state involving mainly the promotion of an

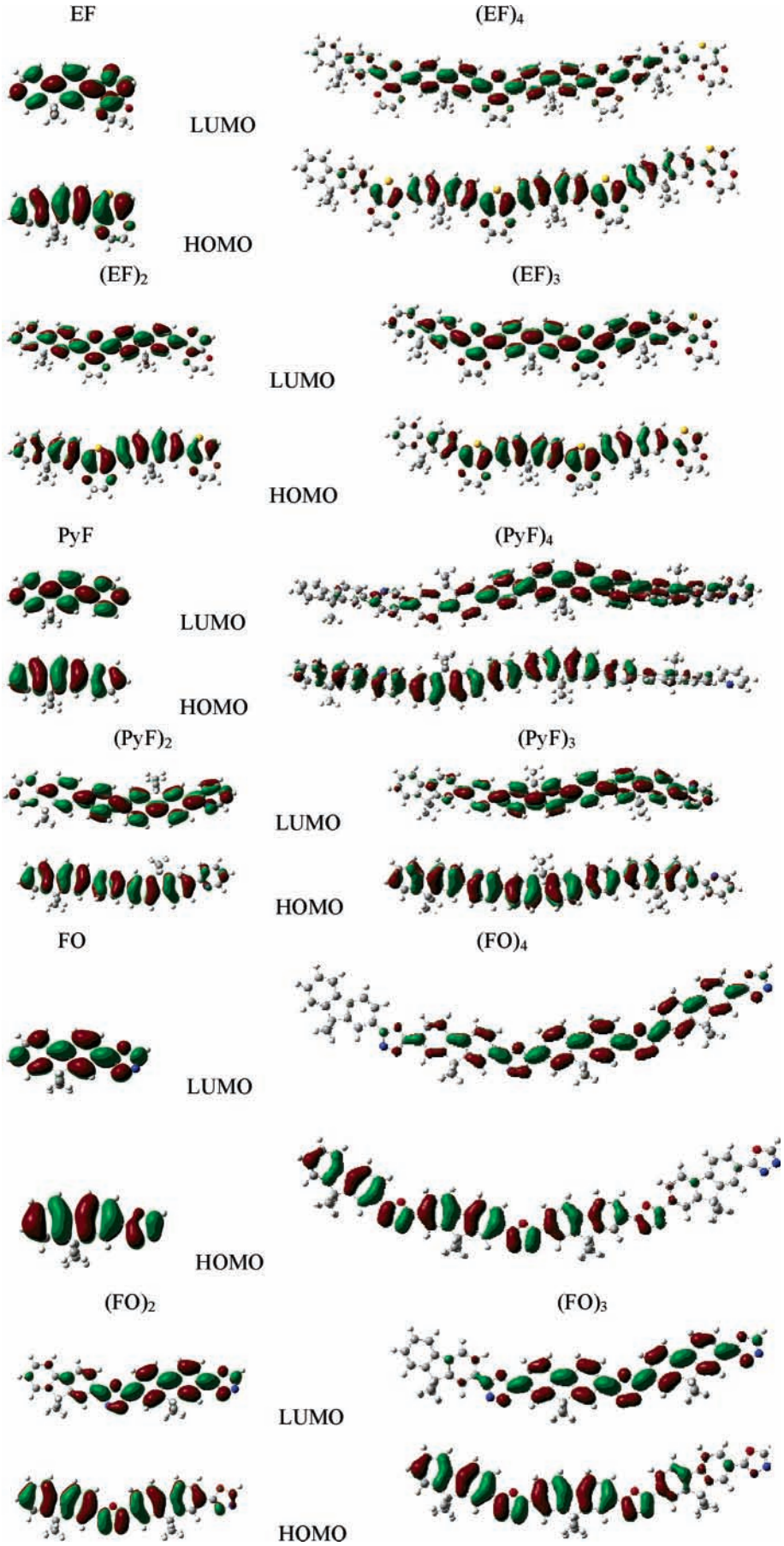

Figure 3. B3LYP/6-31G(d) electronic density contours of the frontier orbitals for $(EF)_n$, $(PyF)_n$, and $(FO)_n$ ($n = 1\sim4$).

electron from the HOMO to the LUMO should be more planar. In PEF, the localization of the electronic cloud distributing in

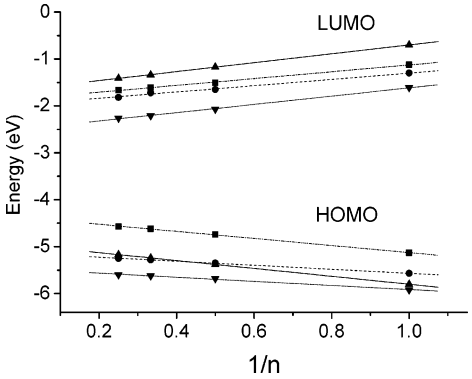

Figure 4. B3LYP/6-31G(d) calculated HOMO and LUMO energies of PEF (▲), PPyF (●), PFO (▼), and PF (■) oligomers as a function of the inverse number of monomer units.

the middle part of the oligomer is typically expected due to chain-end effects. In contrast, asymmetric character prevails for both the HOMO and LUMO when 2,5-ethylenedioxythiophene units are replaced by pyridine and 1,3,4-oxadiazole units, and this character is gradually obvious with the increasing oligomer chain length (especially in PFO). As shown in Figure 3, the HOMO remains delocalized on the left parts of the conjugated backbone; the shapes of the LUMOs become different, being localized on the right parts, as a result of the electron-withdrawing property of pyridine and 1,3,4-oxadiazole. One particularly striking difference between $(PyF)_n$ and $(FO)_n$ is that the former is nonplanar whereas the latter is highly planar.

In experiment, the HOMO and LUMO energies were calculated from one empirical formula proposed by Brédas et al.,[13] based on the onset of the oxidation and reduction peaks measured by cyclic voltammetry, assuming the absolute energy level of ferrocene/ferrocenium to be 4.8 eV below vacuum. The HOMO and LUMO energies can be calculated by density functional theory (DFT) in this study. However, it is noticeable that solid-state packing effects are not included in the DFT calculations, which tends to significantly reduce the torsion angles between adjacent units and consequently affects the HOMO and LUMO energy levels in a thin film compared to an isolated molecule as considered in the calculations. Even if these calculated HOMO and LUMO energy levels are not accurate, it is possible to use them to get information by comparing similar polymers and oligomers.

Figure 4 describes the evolution of the B3LYP/6-31G(d) calculated highest occupied molecular orbital (HOMO) and lowest unoccupied molecular orbital (LUMO) energies as a function of the inverse number of monomer units in $(EF)_n$, $(PyF)_n$, and $(FO)_n$. For the sake of comparison, the frontier energy levels of $(F)_n$ ($n = 1\sim4$) are also listed in Figure 4. As is usual in π-conjugated systems, the energy of the frontier electronic levels evolves linearly with inverse chain length in the four systems: the HOMO energies increase, whereas the LUMO energies decrease.[39] Similar energies are obtained for the HOMO of PPyF (−5.3 eV) and PF (∼−5.2 eV)[36] oligomers. The introduction of electron-withdrawing oxadiazole unit slightly lowers the HOMO of PFO (−5.6 eV), whereas the electron-donating EDOT unit significantly lifts the HOMO of the longest oligomer of PEF (−4.6 eV) by some 0.6 eV compared to PF, indicating much improved hole-accepting properties by introduction of the electron-donating moiety EDOT. Turning to the evolution of the LUMO levels, the LUMO energies of PEF (−1.6 eV), PPyF (−1.7 eV), and PFO (−2.2 eV) are generally stabilized by about 0.3, 0.4, and 0.9 eV with respective to PF (∼−1.3 eV) chains due to the incorporation of the charge carriers. This indicates that the combination with electron-donating and -withdrawing moieties will both lower the LUMO energies. The more planar conformations in the three series under study relative to PF are also the reasons. Since the HOMO shows interring antibonding character and the LUMO shows interring bonding character, the variation of torsional angles should have larger effects on LUMO. Indeed, the decrease in the dihedral angles between the two adjacent subunits induced by the presence of the electron-donating moiety EDOT or electron-accepting moieties pyridine and 1,3,4-oxadiazole should enhance the electron conjugation over the whole molecule and thus stabilize the LUMOs. Especially, in the highly planar PFO, the LUMO energy levels are dramatically decreased. Similarly, the large torsional angles in PEF and PPyF relative to PFO also should be responsible for the relatively high LUMO energies in the former two.[46]

3.3. Properties of Ionic States. *3.3.1. Optimized Geometries in Ionic States.* As already mentioned, one of the most important features of the π-conjugated polymers is their ability to become highly conducting after oxidative (p-type) or reductive (n-type) doping. So, the cationic and anionic geometries of oligomers in all series of $(EF)_n$, $(PyF)_n$, and $(FO)_n$ ($n = 1-4$) were optimized by B3LYP/6-31G(d), and interring bond lengths and dihedral angles are compiled in Table 2. DFT calculations are known to give a more delocalized charge distribution for charged conjugated oligomers than INDO/s-CIS or HF calculations. A possible explanation presented by Siebbeles and co-workers[47−50] for the higher degree of delocalization in DFT is the presence of electron correlation. They pointed out that the two methods are developed from different monoelectronic operators with different theoretical frameworks. DFT includes the electron correlation, whereas in INDO/s-CIS calculations, the dynamic correlation is not taken into consideration. The extent to which electron correlation is taken into consideration has a large effect on the delocalization of excess charge. They also pointed out that the DFT results suggest that the existence of localized charges in solids should be attributed to impurities or defects in the films or crystals. These defects can be of a chemical nature, such as polymerization mistakes causing cross-links or broken conjugation. Moreover, the localization of charges can be induced by conformational defects caused by interchain interactions. However, it has also been suggested that the delocalization in DFT is an artifact due to the approximate description of the exchange interaction. To gain insight into the effects of the exchange part of the functional on the charge delocalization, Fratiloiu et al.[47] employed BLYP and B3LYP to calculate charge distributions. The results show that the effect of improving the description of the exchange interaction does not lead to a significant localization of the charge. They think that the presence of electron correlation is responsible for the increased delocalization of the charge.

From Table 2, it can be seen that the geometry deformations of the positively and negatively charged copolymers of all systems were found to be evenly spread over the entire chain, which indicates that, according to DFT, no self-localized polaron is formed. This is analogous to the DFT results for positively charged oligo(phenylene vinylene)s[49] and oligo(thienylene vinylene)s[50] and negatively charged oligo(phenylene vinylene)s.[47] The maximum changes in interring bond length due to adding an electron or a hole were found to be ∼0.01 Å for the three systems. In contrast with the present findings, Ye et al.[51] showed that for an AM1 optimized geometry there is a significant modification in the conformation of the PV chain when an

TABLE 2: Selected Important Interring Dihedral Angles and Distances of $(EF)_n$, $(PyF)_n$, and $(FO)_n$ ($n = 1\sim4$) in the Cationic and Anionic States Obtained by B3LYP/6-31G(d) Calculations

		cationic							anionic						
$(EF)_n$		F−T	T−F	F−T	T−F	F−T	T−F	F−T	F−T	T−F	F−T	T−F	F−T	T−F	F−T
$n = 1$	r	1.422							1.421						
	Φ	1.6							3.0						
$n = 2$	r	1.436	1.431	1.442					1.432	1.429	1.445				
	Φ	3.4	1.1	3.9					2.2	2.1	6.3				
$n = 3$	r	1.445	1.439	1.438	1.440	1.449			1.442	1.439	1.438	1.439	1.451		
	Φ	5.3	2.9	2.1	3.4	5.2			3.1	3.2	2.7	3.1	7.9		
$n = 4$	r	1.456	1.456	1.456	1.456	1.456	1.456	1.458	1.446	1.445	1.443	1.443	1.444	1.444	1.453
	Φ	8.5	7.2	8.2	8.3	8.5	8.4	10.7	4.6	5.1	3.1	2.0	5.3	3.7	9.4

		cationic							anionic						
$(PyF)_n$		F−P	P−F	F−P	P−F	F−P	P−F	F−P	F−P	P−F	F−P	P−F	F−P	P−F	F−P
$n = 1$	r	1.464							1.442						
	Φ	0.0							0.0						
$n = 2$	r	1.460	1.460	1.477					1.461	1.458	1.463				
	Φ	3.4	25.3	1.0					0.7	19.4	0.7				
$n = 3$	r	1.468	1.468	1.470	1.468	1.482			1.471	1.467	1.464	1.466	1.472		
	Φ	0.5	29.5	6.5	27.2	2.0			0.6	25.8	1.4	24.4	2.1		
$n = 4$	r	1.471	1.471	1.473	1.472	1.474	1.472	1.483	1.475	1.471	1.470	1.470	1.469	1.470	1.475
	Φ	5.0	30.3	5.1	30.7	2.7	30.3	7.6	2.3	27.9	1.2	28.1	2.2	26.9	0.9

		cationic							anionic						
$(FO)_n$		F−O	O−F	F−O	O−F	F−O	O−F	F−O	F−O	O−F	F−O	O−F	F−O	O−F	F−O
$n = 1$	r	1.433							1.411						
	Φ	0.0							0.0						
$n = 2$	r	1.425	1.426	1.445					1.433	1.424	1.428				
	Φ	0.0	0.0	0.0					0.0	0.0	0.0				
$n = 3$	r	1.446	1.435	1.436	1.434	1.432			1.441	1.433	1.433	1.433	1.435		
	Φ	0.0	0.0	0.0	0.0	0.0			0.0	0.0	0.0	0.0	0.0		
$n = 4$	r	1.447	1.439	1.440	1.439	1.439	1.438	1.436	1.443	1.438	1.438	1.438	1.437	1.437	1.438
	Φ	0.0	0.0	0.0	0.0	0.0	0.0	0.0	0.0	0.0	0.0	0.0	0.0	0.0	0.0

[a] F means the fluorene ring; T is the 2,5-ethylenedioxythiophene; P is the pyridine; O is the 1,3,4-oxadiazole in every molecule.

electron is added. In this case, the lattice distortions are mostly located around the center of the chain, indicating the formation of a self-localized polaron. Recently, Grozema et al.[50] found the geometry deformations in the DFT calculations are evenly spread over the whole PV chain and exhibit no features characteristic of the formation of a self-localized polaron, in contrast to the earlier AM1 Results. Similar differences between DFT and HF calculations have been found for thiophene oligomers. Moro et al.[52] have performed DFT geometry optimizations for thiophenes and also found that the geometry deformation was evenly spread over the entire oligomer while earlier AM1[53] calculations yielded a polaron localized on five thiophene rings. For thiophene oligomers, calculations by Brédas and co-workers[54,55] at the MP2 level seem to indicate that the delocalization in DFT is an artifact; however, it was also shown that the MP2 geometry deformation for a singly charged oligothiophene is more delocalized than the HF geometry deformation. It would be of interest to establish whether the larger delocalization of the charge in DFT calculations is an artifact of the method or a real physical phenomenon. To resolve this issue, more experimental data on long oligomers, for example, by ESR measurements, and calculations by other methods, for example, MP2 calculations, are called for.[56]

Comparing the results in Table 1 with Table 2, we found that the interring distances between the two adjacent units decrease in both the cationic and anionic states in both series. The shortening of the interring distances in ionic states relative to that in the neutral state can easily be seen from the HOMO and LUMO characters plotted in Figure 3. There is interring antibonding between the bridge atoms, and there is intraring bonding between the bridge carbon atom and its conjoined atoms in the HOMO. Hence, removing an electron from HOMO leads to a shortening of the interring distances in the cationic state relative to the neutral state. On the other hand, the LUMO of all the oligomers generally shows bonding character between the two adjacent subunits. The shortening of the interring distance in the anionic state is due to the bonding interactions between the π orbitals on the two adjacent phenyls or thienyls. On the other hand, the injection of electrons or holes in these oligomers of all series induces better conjugation than their corresponding neutral ground states. The dihedral angles between subunits of each oligomer in cationic and anionic states obviously decrease compared with their corresponding neutral states. Of course, with an initial highly planar geometry in the oligomers of $(PFO)_n$, the final geometry in ionic states is always planar regardless of charge. In the anionic states of $(EF)_n$ and $(PyF)_n$, the interring torsional angles are around 4° and 27°, even smaller than in their cationic states. This indicates that the whole molecules tend to be more planar with the injection of electrons or holes in these oligomers.

3.3.2. Ionization Potentials and Electron Affinities. The adequate and balanced transport of both injected electrons and holes is important in optimizing the performance of OLED devices. The ionization potential (IP) and electron affinity (EA) are well-defined properties that can be calculated by DFT on the geometries in the neutral, cationic, and anionic sates to estimate the energy barrier for the injection of both holes and electrons into the polymer. Table 3contains the ionization potentials and electron affinities, both vertical (v; at the geometry of the neutral molecule) and adiabatic (a; optimized structure for both the neutral and charged molecule), and extraction potentials (HEP and EEP for the hole and electron, respectively) that refer to the geometry of the ions.[57−59] The IP, EA, HEP, and EEP for infinite chains of the polymers were determined by plotting these values of oligomers against the reciprocal of

TABLE 3: Ionization Potentials, Electron Affinities, and Extraction Potentials for Each Molecule[a]

	IP(v)[b]	IP(a)[b]	HEP	EA(v)[b]	EA(a)[b]	EEP
			$(EF)_n$			
$n=1$	6.73	6.71	6.41	0.17	0.18	0.60
$n=2$	5.96	6.04	5.70	0.86	0.89	1.24
$n=3$	5.68	5.76	5.45	1.11	1.25	1.46
$n=4$	5.45	5.67	5.43	1.33	1.38	1.62
$n=\infty$	5.10	5.30	5.04	1.63	1.75	1.92
			$(PyF)_n$			
$n=1$	7.23	7.12	6.98	0.32	0.48	0.68
$n=2$	6.62	6.52	6.37	1.00	1.12	1.30
$n=3$	6.27	6.33	6.18	1.28	1.40	1.59
$n=4$	6.16	6.17	6.10	1.40	1.49	1.72
$n=\infty$	5.85	5.90	5.80	1.75	1.81	2.04
			$(FO)_n$			
$n=1$	7.65	7.63	7.43	0.54	0.61	0.94
$n=2$	7.00	7.09	6.80	1.33	1.26	1.64
$n=3$	6.74	6.95	6.61	1.65	1.45	1.90
$n=4$	6.69	6.80	6.55	1.84	1.66	2.18
$n=\infty$	6.35	6.57	6.24	2.21	1.94	2.47

[a] Values are given in electronvolts. [b] (v) and (a) indicate vertical and adiabatic values, respectively.

the number of modeling polymeric units and by extrapolating the number of units to infinity.

One major problem with PFs for applications in OLEDs is that they are not good charge acceptors. However, this drawback has been modified by the modification of the chemical structures. Similarly, we employ PF as comparison. The reported value required to create a hole in PF is ~5.4 eV,[34] which is lower than that of PPyF (~5.8 eV) and PFO (~6.3 eV), and it is higher by around 0.3 eV than that in PEF (~5.1 eV), suggesting that in PEF it is easier to create a hole than in the other two polymers and PF, which is consistent with the analysis for HOMO energy. The extraction of an electron from the anion requires ~1.2 eV in PF,[34] which is lower than all three copolymers under study. This indicates that the combination with electron-donating or -accepting moieties will improve both the electron-accepting ability and the order of 1.76 (PEF) < 1.86 (PPyF) < 2.21 eV (PFO) and exhibits that electron-accepting moieties or the more planar conformations are more in favor of accepting electrons. It is clear from these results that the introduction of electron-donating or -accepting moieties allows the modulation of the ionization potential and electron affinity. This should be useful to enhance the injection of holes and electron-transport from anode and cathode in light-emitting diodes.

3.4. HOMO-LUMO Gaps and the Lowest Excitation Energies. There are two theoretical approaches for evaluating the energy gap in this paper. One way is based on the ground-state properties, from which the energy gap is estimated from the energy difference between the highest occupied molecular orbital (HOMO) and the lowest unoccupied molecular orbital (LUMO) when $n = \infty$, termed the HOMO−LUMO gaps (Δ_{H-L}).[60−62] TD-DFT, which has been used to study systems of increasing complexity due to its relatively low computational cost and also to include in its formalism the electron correlation effects, is also employed to extrapolate the energy gap of polymers from the calculated first dipole-allowed excitation energy of their oligomers.

Here, the HOMO−LUMO gaps (Δ_{H-L}) and lowest singlet excited energies (E_g) are both listed in Table 4, and the relationships between the calculated Δ_{H-L}, E_g, and the inverse chain length are plotted in Figure 5. There is a good linear relationship between the energy gaps by both methods and the inverse chain length. In fact, the theoretical quantity for direct comparison with experimental band gap should be the transition (or excitation) energy from the ground state to the first dipole-allowed excited state. The approach to get band gap from the orbital energy difference between the HOMO and LUMO is crude considering the experimental comparison. The implicit assumption underlying this approximation is that the lowest singlet excited state can be described by only one singly excited configuration in which an electron is promoted from HOMO to LUMO. In addition, the orbital energy difference between HOMO and LUMO is still an approximate estimate to the transition energy since the transition energy also contains significant contributions from some two-electron integrals. However, because the HOMO−LUMO gap is easy to obtain, the approach can also be used to provide valuable information on estimated band gaps of oligomers and polymers, especially treating even larger systems.[63,64] Interestingly, for copolymers studied in this work, however, good agreement between the HOMO−LUMO gaps and experimental observations in all the series has been demonstrated with density functional theory (DFT). Optical band gaps derived from the absorption edge of a polymer thin film for $(EF)_n$, $(PyF)_n$, and $(FO)_n$ are 2.44, 2.87, and 3.03 eV, differing by 0.11, 0.26, and 0.03 eV from our calculated values by HOMO−LUMO gap of 2.55, 3.13, and 3.00 eV, respectively.

As shown in Table 4, the extrapolated energy gaps from TD-DFT excitation energies systematically underestimate the actual band gap derived from the solid-state data due to the inherent limitation in TD-DFT calculations as mentioned in the Introduction.[65,66] Two other factors may also be responsible for deviations by both methods from experimental. One is that the predicted band gaps are for the isolated gas-phase chains, while the experimental band gaps are measured in the liquid phase where environmental influences may be involved. Another factor that should be borne in mind is that solid-state effects (like polarization effects and intermolecular packing forces) have been neglected in the calculations. The latter can be expected to result in a decreased interring twist and consequently a reduced gap in a thin film compared to an isolated molecule as considered

TABLE 4: HOMO−LUMO Gaps by DFT and the Lowest Excitation Energies by TD-DFT in Oligomers of $(EF)_n$, $(PyF)_n$, and $(FO)_n$ ($n = 1-4$)[a]

$(EF)_n$			$(PyF)_n$			$(FO)_n$		
oligomer	Δ_{H-L}	E_g (TD)	oligomer	Δ_{H-L}	E_g (TD)	oligomer	Δ_{H-L}	E_g (TD)
$n=1$	4.01	3.87	$n=1$	4.27	4.15	$n=1$	4.31	4.28
$n=2$	3.24	2.99	$n=2$	3.71	3.41	$n=2$	3.61	3.32
$n=3$	3.01	2.76	$n=3$	3.52	3.21	$n=3$	3.42	3.11
$n=4$	2.91	2.66	$n=4$	3.43	3.09	$n=4$	3.34	3.03
$n=\infty$	2.55	2.21	$n=\infty$	3.13	2.76	$n=\infty$	3.00	2.58
expl	2.44[b]	2.38[c]	expl	2.87[b]	2.69[c]	expl	3.03[b]	

[a] HOMO−LUMO gaps and excitation energies are given in electronvolts. [b] Optical band gap derived from the absorption edge of a polymer thin film; [c] Derived from the electrochemical method.

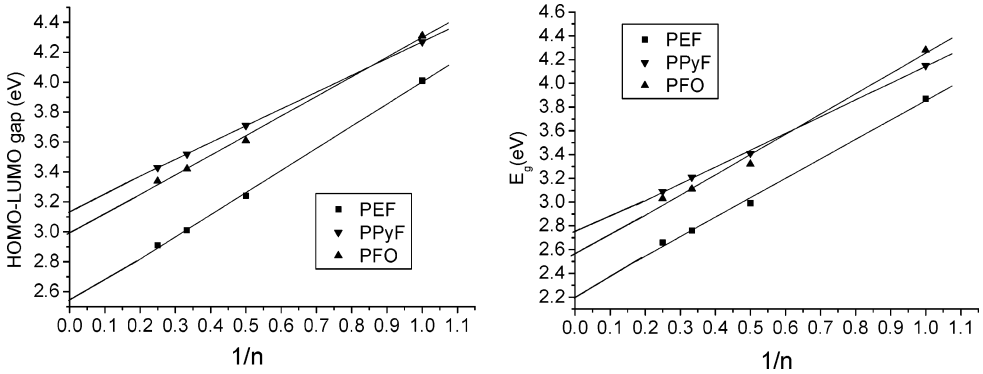

Figure 5. HOMO−LUMO gaps (Δ_{H-L})s by B3LYP and the lowest excitation energies E_g by TD-DFT as a function of reciprocal chain length n in oligomers of $(EF)_n$, $(PyF)_n$, and $(FO)_n$.

in the calculations.[67,68] The better agreement between the HOMO−LUMO gap and the experimental observations in the highly planar copolymer PFO than the other two systems may be attributed to the solid-state effects. Even with these discrepancies between the calculated and experimental data, it is possible to use them to get information by comparing similar polymers or molecules.

As mentioned above, our main interest in the study of the energy gaps relative to PF is to see the influence of electron-donating moiety EDOT and electron-accepting moieties pyridine and 1,3,4-oxadiazole onto fluorene. The band gaps obtained by HOMO−LUMO gaps and TD-DFT are 3.33 and 2.91 eV for PF,[34] respectively, which are both higher than those of PEF, PPyF, and PFO with the same corresponding methods, indicating that either electron-donating groups (EDOT) or electron-accepting moieties (pyridine and 1,3,4-oxadiazole) narrow the band gaps of fluorene-based copolymers. Furthermore, on all accounts, the results of both methods indicate that the energy gaps in PPyF are larger than that of PFO. It can be concluded that the breaking of the conjugation in the backbone will broaden the energy gap, and on the contrary, the good π-conjugated conformation should narrow the energy gap. As one can see, the variation trend of PFO does not agree with the experimental observations, which indicates that the energy gap of PFO is larger than that of PPyF. In fact, our previous calculations[34,43c] (the results agree well with the experimental data) on similar fluorene-containing systems also support the conclusions in this paper that decreasing conjugation in the backbone broadens the band gap and vice versa. More experimental data are called for to test the calculated results.

3.5. Absorption Spectra. TD-DFT//B3LYP/6-31G(d) and ZINDO have been used on the basis of the optimized geometry to obtain the nature and the energy of the singlet−singlet electronic transitions of all the oligomers in all series under study. Here, we list the transition energies, oscillator strengths, configurations, and transition dipole moments obtained by TD-DFT and ZINDO calculations for the most relevant first five singlet excited states in each oligomer of $(EF)_n$, $(PyF)_n$, and $(FO)_n$ in Tables S3−S5 of the Supporting Information.[69] As shown in Tables S3−S5, all electronic transitions are of the $\pi-\pi^*$ type and involve both subunits of the molecule. In other words, no localized electronic transitions are calculated among the first three singlet−singlet transitions. Both methods show that excitation to the S_1 state corresponds almost exclusively to the promotion of an electron from the HOMO to the LUMO. The oscillator strength (×c4) and the transition dipole moment along the long axis of the molecule (χ) of the S0 → S1 electronic transition are overwhelmingly the largest in each oligomer relative to the next four excited states. Considering the fact that the oscillator strength is proportional to the square of the transition moment, it is reasonable that the S0 → S1 transition show a large ×c4 value. Furthermore, the oscillator strength coupling the lowest $\pi-\pi^*$ singlet excited state to the ground state increases strongly when going from an isolated molecule to a molecular group. The oscillator strength associated with the S_1 state increases by about 1 order of magnitude upon addition of one repeated unit to the monomers in all series.

Obviously, the strongest absorption peaks are all assigned to $\pi-\pi^*$ electronic transition character arising exclusively from $S_0 \rightarrow S_1$ electronic transition mainly composed by HOMO → LUMO transition. In fact, there are similar characters and variation trends in $(EF)_n$ and $(PyF)_n$ as in the cases of $(FO)_n$. We find in Tables S3−S5 that, with the conjugation lengths increasing, the absorption wavelengths increase progressively as in the case of the oscillator strengths of the $S_0 \rightarrow S_1$ electronic transition. This is reasonable, since the HOMO → LUMO transition is predominant in the $S_0 \rightarrow S_1$ electronic transition and, as analysis above showed, that with increasing molecular size the HOMO−LUMO gaps decrease. Since the first allowed transitions are also the absorption maxima, they have the same variation trend, which needs no further elaboration.

3.6. Properties of Excited Structures and Emission Spectra. Up to now, the standard for calculating excited-state equilibrium properties of larger molecules in the Gaussian program package is the configuration interaction singles (CIS) method. However, due to the neglect of electron correlation, CIS results are not accurate enough in many applications. In this study, we hope to investigate the excited-state properties by this method, despite the inaccuracy. Because the calculation of excited-state properties typically requires significantly more computational effort than is needed for the ground states and is dramatically constrained by the size of the molecules, we optimize only the monomers for PEF and PPyF and PFO, in view of the molecular weights, by CIS/6-31G(d) and compare with their ground structures by HF/6-31G(d). Interestingly, the main character of the frontier orbitals by HF/6-31G(d) is the same as by B3LYP/6-31G(d). We compare only the excited structures of EF and FO by CIS/6-31G(d) with their ground structures by HF/6-31G(d) for the sake of comparison as shown in Figure 6.

As shown, some of the bonds lengthened, but some shortened. In fact, we can predict the differences in the bond lengths between the ground (S_0) and singlet excited state (S_1) from MO nodal patterns. Due to the singlet state corresponding to an excitation from the HOMO to the LUMO in all considered series, we explore the bond length variations by analyzing the HOMO and LUMO. By comparison of Figure 6 with Figure 3, the HOMO has nodes across $r(2,3)$, $r(5,6)$, $r(2',3')$, $r(5',6')$,

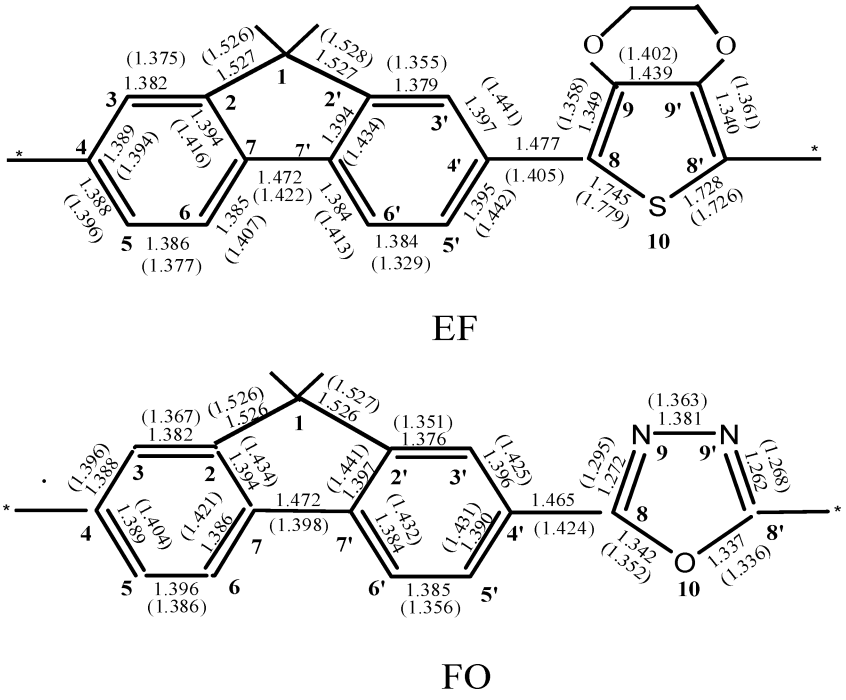

Figure 6. Comparison of the excited structure (values in parentheses) by CIS/6-31G(d) with the ground geometry by HF/6-31G(d) for the monomers of PEF and PFO.

r(7′,7), *r*(9′,9), and *r*(4′,8) bonds in both EF and FO, but the LUMO is bonding in these regions. Therefore one would expect contraction of these bonds; the data in the figure show that these bonds are in fact considerably shorter in the excited state. The LUMO has a node across the *r*(3,4), *r*(2,7), *r*(7,6), *r*(3′,4′), *r*(4′,5′), *r*(2′,7′), *r*(7′,6′), *r*(8′,9′), and *r*(8,9) bonds in both EF and FO while the HOMO is bonding. The data confirm the anticipated elongation of these bonds.

The dihedral angle Φ(3′,4′,8,9) decreases from 36° to 1.2° and from 32° to 0.02° in EF and PyF, respectively; that is, *r*(4′,8) rotates during excitation, and FO still keeps a high-planar conformation. It is obvious that the excited structure has a strong coplanar tendency in all series; in other words, the conjugation is better in the excited structure, which is consistent with the estimation from the character of the frontier orbitals.

On the excited geometries optimized by ab initio CIS, the emission wavelengths are computed by ZINDO and TD-DFT for monomers of PEF, PPyF, and PFO. As in the case of the absorption spectra, both methods reflect that the oligomeric λ_{em} exhibits a red shift compared with monomer fluorene, 270.60 < 319.19 < 335.24 < 354.20 nm (TD-DFT) and 295.6 < 336.6 < 347.7 < 389.8 nm (ZINDO), going from F to FO to PyF to EF, which is consistent with the trend of our calculated energy gaps. Furthermore, similar to absorption spectra, the emission peaks with strongest oscillator strength are all assigned to $\pi-\pi^*$ character arising from S_1, HOMO to LUMO transition. Although there are some discrepancies between the calculated values and the observed data, they show again the effects on the properties by electron-donating or -withdrawing moieties. Most importantly, pure deep strong blue electronluminescence was successfully achieved from these copolymers.[24,25]

4. Conclusion

All the oligomers investigated show less twisted structures compared with pristine polyfluorene by incorporation ofelectron-donating 3,4-ethylenedioxythiophene (EDOT) or electron-withdrawing pyridine and 1,3,4-oxadiazole moieties. All decisive molecular orbitals are delocalized on both subunits of the oligomers. The HOMO possesses antibonding character between subunits, which may explain the nonplanarity observed for these oligomers in their ground state. On the other hand, the LUMO shows bonding character between the two adjacent rings, in agreement with the more planar S_1 excited state. The advantage of the three series of oligomers and polymers under study is that the insertion of electron-donating or -accepting functional groups has allowed modification of the chemical structures to achieve both efficient charge injection and balanced mobility of both charge carriers inside the EL materials, thus obtaining the high quantum efficiency EL devices. The combination of electron-donating unit EDOT with the fluorene moiety resulted in raised HOMO energies and consequently the hole injection was greatly improved. However, even though both kinds of charge carriers will improve the electron-accepting ability, the results show that electron-accepting moieties will greatly facilitate the electron-transporting. The more planar conformation is another reason. The highly planar structural character in PFO resulting from the strong push−pull effect between the fluorene ring and the 1,3,4-oxadiazole ring and a weak interaction between the nitrogen and oxygen atoms in 1,3,4-oxadiazole ring and the hydrogen atom of the fluorene ring significantly improve the electron-accepting and transporting properties by the low LUMO energy levels. Excitation to the S_1 state corresponds almost exclusively to the promotion of an electron from the HOMO to the LUMO. Accordingly, the energy of the $S_0 \rightarrow S_1$ electronic transition follows the HOMO−LUMO energy gap of each oligomer. The first electronic transition gives rise to the largest values of the oscillator strength in each oligomer. The absorption and emission spectra of the alternating copolymers were red-shifted with the addition of the electron-donating EDOT or electron-accepting pyridine and 1,3,4-oxadiazole moieties, especially by incorporation with the EDOT content.

Finally, this theoretical study confirmed experimental results, where it was shown that the incorporated copolymers could greatly modulate and improve the electronic and optical properties of pristine polymers. Furthermore, using theoretical

methodologies, we showed that is possible to predict reasonably the electronic properties of conjugated systems, and we are convinced that the systematic use of those theoretical tools should contribute to orientate the synthesis efforts and help understand the structure−properties relation of these conjugated materials.

Acknowledgment. This work is supported by the Major State Basis Research Development Program (2002CB 613406) and the National Nature Science Foundation of China (90101026) and the Key Laboratory for Superamolecular Structure and Material of Jilin University.

Supporting Information Available: Tables showing the negative of HOMO and LUMO energies for $(EF)_n$ and $(PyF)_n$, Mulliken atomic charge distributions in positively and negatively charged oligomer $(FO)_3$, and electronic transition data for $(EF)_n$, $(PyF)_n$, and $(FO)_n$. This material is available free of charge via the Internet at http://pubs.acs.org.

References and Notes

(1) Kraft, A.; Grimsdale, A. C.; Holmes, A. B. *Angew. Chem., Int. Ed.* **1998**, *37*, 402−428.
(2) Mitschke, U.; Bäuerle, P. *J. Mater. Chem.* **2000**, *10*, 1471−1507.
(3) Dimitrakopoulos, C. D.; Malenfant, P. R. L. *Adv. Mater.* **2002**, *14*, 99−117.
(4) Garnier, F.; Hajlaoui, R.; Yassar, A.; Srivastava, P. *Science* **1994**, *265*, 1684.
(5) Lovinger, A. J.; Rothverg, L. *J. Mater. Res.* **1996**, *11*, 1581.
(6) Bao, Z.; Lovinger, A. J.; Brown, J. *J. Am. Chem. Soc.* **1998**, *120*, 207.
(7) Brabec, C. J.; Sariciftci, N. S.; Hummelen, J. C. *Adv. Funct. Mater.* **2001**, *11*, 15−26.
(8) Leclerc, M.; Faid, D. *Adv. Mater.* **1997**, *35*, 3627.
(9) Ranger, M.; Leclerc, M. *Macromolecules* **1999**, *32*, 3306.
(10) Grem, G.; Leditzky, G.; Ullrich, B.; Leising, G. *Adv. Mater.* **1992**, *4*, 36.
(11) Weiss, H.; Steiger, S.; Jungling, S.; Yakimansky, A. V.; Muller, A. H. E. *Macromolecules* **2003**, *36*, 3374−3379.
(12) Mushrush, M.; Facchetti, A.; Lefenfeld, M.; Katz, H. E.; Marks, T. J. *J. Am. Chem. Soc.* **2003**, *125*, 9414−9423.
(13) Brédas, J. L.; Silbey, R.; Boudreaux, D. S.; Chance, R. R. *J. Am. Chem. Soc.* **1983**, *105*, 6555−6559.
(14) Tavan, P.; Schulten, K. *J. Chem. Phys.* **1986**, *85*, 6602−6609.
(15) Beljonne, D.; Shuai, Z.; Cornil, J.; dos Santos, D. A.; Bredas, J. L. *J. Chem. Phys.* **1999**, *32*, 267−276.
(16) Lahti, P. M.; Obrzut, J.; Karasz, F. E. *Macromolecules* **1987**, *20*, 2023−2026.
(17) Burrows, H. D.; Seixas de Melo, J.; Serpa, C.; Arnaut, L. G.; Miguel, N. da G.; Monkman, A. P.; Hamblett, I.; Navaratnam, S. *J. Chem. Phys.* **2002**, *285*, 3−11.
(18) Scheinert, S.; Schliefke, W. *Synth. Met.* **2003**, *139*, 501−509.
(19) Salzner, U.; Lagowski, J. B.; Pickup, P. G.; Poirier, R. A. *Synth. Met.* **1998**, *96*, 177−189.
(20) Oyaizu, K.; Iwasaki, T.; Tsukahara, Y.; Tsuchida, E. *Macromolecules* **2004**, *37*, 1257.
(21) Peng, Q.; Lu, Z. Y.; Huang, Y.; Xie, M. G.; Han, S. H.; Peng, J. B.; Cao, Y. *Macromolecules* **2004**, *37*, 260.
(22) Yang, R. Q.; Tian, R. Y.; Yang, W.; Cao, Y. *Macromolecules* **2003**, *36*, 7453.
(23) Yang, N. C.; Lee, S. M.; Yoo, Y. M.; Kim, J. K.; Suh, D. H. *J. Polym. Sci., Part A: Polym. Chem.* **2004**, *42*, 1058.
(24) Aubert, P. H.; Knipper, M.; Groenendaal, L.; Lutsen, L.; Manca, J.; Vanderzande, D. *Macromolecules* **2004**, *37*, 4087.
(25) Zhang, J. P.; Frenking, G. *J. Phys. Chem. A* **2004**, *108*, 10296−10301.
(26) Briére, J. F.; Côté, M. *J. Phys. Chem. B* **2004**, *108*, 3123−3129.
(27) Ford, W. K.; Duke, C. B.; Paton, A. *J. Chem. Phys.* **1982**, *77* (9), 4564−4572.
(28) Klaerner, G.; and Miller, R. D. *Macromolecules* **1998**, *31*, 2007−2009.
(29) Brébdas, J. L.; Chance, R. R. Silbey, R. *Phys. Rev. B* **1982**, *26*, 5843−5854.
(30) Ma, J.; Li, S. H.; Jiang, Y. S. *Macromolecules* **2002**, *35*, 1109−1115.
(31) Zhang, G. L.; Ma, J.; Jiang, Y. S. *Macromolecules* **2003**, *36*, 2130−2140.
(32) Cao, H.; Ma, J. Zhang, G. L.; Jiang, Y. S. *Macromolecules* **2005**, *38*, 1123−1130.
(33) Zhou, X.; Ren, A. M.; Feng, J. K. *Polymer* **2004**, 7747−7757.
(34) Wang, J. F.; Feng, J. K.; Ren, A. M.; Liu, X. D.; Ma, Y. G.; Lu, P.; Zhang, H. X. *Macromolecules* **2004**, *37*, 3451.
(35) Tozer, D. J.; Handy, N. C. *J. Chem. Phys.* **1998**, *109*, 10180.
(36) Casida, M. E.; Jamorski, C.; Casida, K. C.; Salabub, D. R. *J. Chem. Phys.* **1998**, *108*, 4439.
(37) Gao, Y.; Liu, C.; Jiang, Y. *J. Phys. Chem. A* **2002**, *106*, 5380.
(38) Hsu, C.; Hirata, S.; Martin, H. *J. Phys. Chem. A* **2001**, *105*, 451.
(39) Cornil, J.; Gueli, I.; Dkhissi, A.; Sancho-Garcia, J. C.; Hennebicq, E.; Calbert, J. P.; Lemaur, V.; Beljoone, D.; Brédas, J. L. *J. Chem. Phys.* **2003**, *118*, 6615−6623.
(40) Frisch, M. J.; Trucks, G. W.; Schlegel, H. B.; Scuseria, G. E.; Robb, M. A.; Cheeseman, J. R.; Montgomery, J. A., Jr.; Vreven, T.; Kudin, K. N.; Burant, J. C.; Millam, J. M.; Iyengar, S. S.; Tomasi, J.; Barone, V.; Mennucci, B.; Cossi, M.; Scalmani, G.; Rega, N.; Petersson, G. A.; Nakatsuji, H.; Hada, M.; Ehara, M.; Toyota, K.; Fukuda, R.; Hasegawa, J.; Ishida, M.; Nakajima, T.; Honda, Y.; Kitao, O.; Nakai, H.; Klene, M.; Li, X.; Knox, J. E.; Hratchian, H. P.; Cross, J. B.; Adamo, C.; Jaramillo, J.; Gomperts, R.; Stratmann, R. E.; Yazyev, O.; Austin, A. J.; Cammi, R.; Pomelli, C.; Ochterski, J. W.; Ayala, P. Y.; Morokuma, K.; Voth, G. A.; Salvador, P.; Dannenberg, J. J.; Zakrzewski, V. G.; Dapprich, S.; Daniels, A. D.; Strain, M. C.; Farkas, O.; Malick, D. K.; Rabuck, A. D.; Raghavachari, K.; Foresman, J. B.; Ortiz, J. V.; Cui, Q.; Baboul, A. G.; Clifford, S.; Cioslowski, J.; Stefanov, B. B.; Liu, G.; Liashenko, A.; Piskorz, P.; Komaromi, I.; Martin, R. L.; Fox, D. J.; Keith, T.; Al-Laham, M. A.; Peng, C. Y.; Nanayakkara, A.; Challacombe, M.; Gill, P. M. W.; Johnson, B.; Chen, W.; Wong, M. W.; Gonzalez, C.; Pople, J. A. Gaussian 03, Revision B.04; Gaussian, Inc.: Pittsburgh, PA, 2003.
(41) Foresman, J. B.; Head-Gordon, M.; Pople, J. A. *J. Phys. Chem.* **1992**, *96*, 135.
(42) Belletête, M.; Beaypré, S.; Bouchard, J.; Blondin, P.; Leclerc, M.; Durocher, G. *J. Phys. Chem. B* **2000**, *104*, 9118.
(43) (a) Yang, L.; Ren, A. M.; Feng, J. K.; Liu, X. D.; Ma, Y. G.; Zhang, H. X. *Inorg. Chem.* **2004**, 43, 5961. (b) Yang, L.; Ren, A. M.; Feng, J. K.; Ma, Y. G.; Zhang, M.; Liu, X. D.; Shen, J. C.; Zhang, H. X. *J. Phys. Chem.* **2004**, *108*, 6797. (c) Yang, L.; Ren, A. M.; Feng, J. K. *J. Comput. Chem.* **2005**, *26*, 969.
(44) Ford, W. K.; Duke, C. B.; Salaneck, W. R. *J. Chem. Phys.* **1982**, *77*, 5030.
(45) Marcos, A. D. O.; Duarte, H. A.; Pernaut, J. M.; Wagner, B. D. A. *J. Phys. Chem. A* **2000**, *104*, 8256−8262.
(46) To better investigate the effects of the electron-donating or -withdrawing groups on the energy level excluding the influences of dihedral angles, we have reoptimized the oligomers $(EF)_n$ and $(PyF)_n$ ($n = 3$) as representative example of the whole series of oligomers restricted to fully planar conformations to explain effects coming from the introduction of the electron-donating and -accepting moieties. The negative of HOMO and LUMO energies ($-\epsilon_{HOMO}$ and $-\epsilon_{LUMO}$, in electronvolts) of $(EF)_n$ and $(PyF)_n$ ($n = 3$) obtained by DFT//B3LYP/6-31G* with nonplanar and planar conformations are listed in Table S1 in the Supporting Information. From the calculated results in Table S1, the following can be found: (1) For both $(EF)_3$ and $(PyF)_3$, the planar conformation is much less stable than the nonplanar conformation by 236.20 and 235.89 au, respectively, rationalizing the nonplanar conformations in our paper. (2) The energy levels and the variation trend of HOMO in all systems with fully planar conformations do not change much compared with the ones with the nonplanar conformations. (3) In contrast to the energy level of HOMO, an interesting phenomenon can be found that the LUMO energy of $(EF)_3$ dramatically decreases, even lower than that of $(PyF)_3$ and $(FO)_3$, which indicates that electron-donating groups significantly facilitate the electron-transporting. The results seem to be contrary to the conclusion in the paper. This contradiction can be explained by the effects coming from the torsional angles. Due to the bonding character between the two adjacent subunits, the increasing torsional angles thus destabilize the energy level of LUMO. This interesting phenomenon will be further discussed in a future paper due to space limitations. However, the general conclusion that either the electron-donating or -withdrawing groups will facilitate the electron-transporting is accordant on the basis of either the planar or the nonplanar conformations.
(47) Fratiloiu, S.; Grozema, F. C.; Siebbeles, L. D. A. *J. Phys. Chem. B* **2005**, *109*, 5644−5652.
(48) Fratiloiu, S.; Candeias, L. P.; Grozema, F. C.; Wildeman, J.; Siebbeles, L. D. A. *J. Phys. Chem. B* **2004**, *108*, 19967−19975.
(49) Grozema, F. C.; Candeias, L. P.; Swart, M.; van Duijnen, P. T.; Wildeman, J.; Hadziioanou, G.; Siebbeles, L. D. A.; Warman, J. M. *J. Chem. Phys.* **2002**, *117*, 11366.
(50) Grozema, F. C.; van Duijnen, P. T.; Siebbeles, L. D. A.; Goosens, A.; de Leeuw, S. W. *J. Phys. Chem. B* **2004**, *108*, 16139.
(51) Ye, A.; Shuai, Z.; Kwon, O.; Brédas, J. L.; Beljoone, D. *J. Chem. Phys.* **2004**, *121*, 5567.

(52) Moro, G.; Scalmani, G.; Cosentino, U.; Pitea, D. *Synth. Met.* **2000**, *108*, 165.

(53) Cornil, J.; Beljoone, J.; Brédas, J. L. *J. Chem. Phys.* **1995**, *103*, 842.

(54) Geskin, V. M.; Dkhissi, A.; Brédas, J. L. *Int. J. Quantum Chem.* **2003**, *91*, 350.

(55) (a) Geskin, V. M.; Brédas, J. L. *ChemPhysChem.* **2003**, *4*, 498. (b) Moro, G.; Scalmani, G.; Cosentino, U.; Pitea, D. *Synth. Met.* **2000**, *108*, 165.

(56) (a) To gain insight into the effects of the exchange part of the functional on the charge delocalization, we have carried out additional calculations, for example, using representative BLYP and SVWN functionals accompanied with 6-31g* basis set on the positively and negatively charged trimers of $(FO)_n$ compared with B3LYP functional. The results in Table S2 (Supporting Information) show that the differences among the three charge distributions are rather small and the charge is still delocalized over the entire chain. From these results, it can be concluded that the effect of improving the description of the exchange interaction does not lead to a significant localization of the charge. (b) To clearly establish whether this effect of correlation should be responsible to the charge delocalization, we try to use MP2 to optimize the positively and negatively charged oligomers. Unfortunately, we have not been able to optimize the geometries by MP2 methods, even with STO-3G basis set, due to convergence problems of the optimization procedure. So, restricted closed-shell MP2 (ROMP2) calculations are carried out for $(FO)_3$. The single-point calculations are performed at ROMP2/3-21G* level of theory (as shown in Table S2 of the Supporting Information). Obvious localization of charge around the middle of the chain is observed. The results show that the greater delocalization of a charge on a conjugated chain in DFT is an artifact of the method.

(57) Lin, B. C.; Cheng, C. P.; Lao, Z. P. M. *J. Phys. Chem. A* **2003**, *107*, 5241−5251.

(58) Curioni, A.; Boero, M.; Andreoni, W. *Chem. Phys. Lett.* **1998**, *294*, 263−271.

(59) Wang, I.; Estelle, B. A.; Olivier, S.; Alain, I.; Baldeck, P. L. *J. Opt. A: Pure Appl. Opt.* **2002**, *4*, S258−S260.

(60) Hay, P. J. *J. Phys. Chem. A* **2002**, *106*, 1634−1641.

(61) Curioni, A.; Andreoni W.; Treusch, R.; Himpsel, F. J.; Haskal, E.; Seidler, P.; Heske, C.; Kakar, S.; van Buren, T.; Terminello, L. J. *Appl. Phys. Lett.* **1998**, *72*, 1575−1577.

(62) Hong, S. Y.; Kim, D. Y.; Kim, C. Y.; Hoffmann, R. *Macromolecules* **2001**, *34*, 6474−6481.

(63) (a) Rogero, C.; Pascual, J. I.; Gomez-Herrero, J.; Baro, A. M. *J. Chem. Phys.* **2002**, *116*, 832−836. (b) Curioni, A.; Andreoni W. *IBM J. Res. Dev.* **2001**, *45*, 101−113.

(64) Wang, J. L.; Wang, G. H.; Zhao, J. J. *Phys. Rev. B* **2001**, *64*, 205411.

(65) Grimme, S.; Parac, M. *ChemPhysChem* **2003**, *3*, 292.

(66) Ortiz, R. P.; Delgado, M. C. R.; Casado, J.; Hernández, V.; Kim, O. K.; Woo, H. Y.; Navarrete, L. L. *J.*

(67) Puschning, P.; Ambrosch-Draxl, C.; Heimel, G.; Zojer, E.; Resel, R.; Leising, G.; Kriechbaum, M.; Graupner, W. *Synth. Met.* **2001**, *116*, 327.

(68) Eaton, V. J.; Steele, D. *J. Chem. Soc., Faraday Trans.* 2 **1973**, *2*, 1601.

(69) The transition energies, oscillator strengths, configurations, and transition dipole moments obtained by TD-DFT and ZINDO calculations for the most relevant first five singlet excited states in each oligomer of $(EF)_n$, $(PyF)_n$, and $(FO)_n$ are given in Tables S3−S5 of the Supporting Information.